Frontiers in Bioscience Landmark

Front. Biosci. (Landmark Ed) **2023**; 28(8): 159
https://doi.org/10.31083/j.fbl2808159

Original Research

AMPK Mediates Early Activation of the Unfolded Protein Response through a Positive Feedback Loop in Palmitate-Treated Muscle Cells

Jing Gong[1,2,†], Lu Wang[1,†], Wuchen Tao[1,2], Xiangsheng Pang[1,2], Zonghan Liu[1], Shiming Li[1,2], Wenjiong Li[1], Xiaoping Chen[1,2,*], Peng Zhang[1,*]

[1]State Key Laboratory of Space Medicine Fundamentals and Application, China Astronaut Research and Training Center, 100094 Beijing, China
[2]National Key Laboratory of Human Factors Engineering, China Astronaut Research and Training Center, 100094 Beijing, China
*Correspondence: xpchen2009@163.com (Xiaoping Chen); zhangpeng6128@163.com (Peng Zhang)
[†]These authors contributed equally.
Academic Editor: Elisa Belluzzi
Submitted: 15 December 2022 Revised: 19 January 2023 Accepted: 20 February 2023 Published: 7 August 2023

Abstract

Background: Activation of the unfolded protein response (UPR) is closely related to the pathogenesis of many metabolic disorders. Accumulating evidence also shows that UPR and metabolic signaling pathways are interdependent. The AMP-activated protein kinase (AMPK) signal pathway controls the energy balance of eukaryotes. The aim of this study was therefore to investigate the possible interaction between AMPK signaling and UPR in muscle cells exposed to saturated fatty acids, as well as the potential mechanism. **Methods**: The saturated fatty acid palmitate was used to induce UPR in C2C12 myotubes. Compound C or knockdown of AMPKα with short hairpin RNA (shRNA) were used to inhibit the AMPK signaling pathway in palmitate-treated muscle cells. AMPK signaling in myotubes was activated using 5-amino-1-β-D-ribofuranosylimidazole-4-carboxamide (AICAR) or ex229. C2C12 myotubes were pre-treated with taurourdodeoxycholic acid (TUDCA) to inhibit UPR before adding palmitate. Real-time PCR and Western blotting were performed to evaluate the expression of UPR markers and activation of AMPK. **Results**: Palmitate treatment induced UPR in C2C12 myotubes while activating AMPK signaling. Inhibition of the AMPK pathway with compound C or AMPK shRNA reduced palmitate-induced activation of UPR, while inhibition of UPR with TUDCA reduced palmitate-induced AMPK activation. This indicates a positive feedback loop between UPR and AMPK. Furthermore, activation of the AMPK pathway with AICAR or ex229 caused a dose-dependent upregulation of UPR markers, including activating transcription factor 4 (ATF4), binding immunoglobulin protein (BIP), and growth arrest and DNA damage-inducible 34 (GADD34) protein. **Conclusions**: These results provide the first evidence that AMPK signaling is involved in the early activation of UPR caused by saturated fatty acids in skeletal muscle. Furthermore, they indicate that physiological or pharmacological activation of the AMPK pathway (e.g., by exercise or phenformin, respectively) can promote muscle health and function, thereby improving the quality of life in individuals with metabolic disorders due to a high-fat diet or obesity.

Keywords: palmitate; ER stress; unfolded protein response; AMPK; C2C12 myotube

1. Introduction

Adult skeletal muscle shows considerable plasticity that allows it to respond rapidly under a variety of physiologic and pathologic conditions [1]. This is facilitated by the sarcoplasmic reticulum, a specialized form of the endoplasmic reticulum (ER) [2]. Environmental or cell-intrinsic stimuli such as nutrient or oxygen deprivation, exposure to toxic substances, and oxidative stress can disrupt cellular homeostasis and induce ER stress, thereby activating the unfolded protein response (UPR) [3–5]. The canonical UPR in mammals is initiated by activation of three major ER transmembrane sensors: PKR-like endoplasmic reticulum kinase (PERK), activating transcription factor 6 (ATF6), and inositol-requiring enzyme 1 (IRE1) [6–8]. These trigger the expression of downstream transcription factors including ATF4, ATF6c, C/EBP homologous protein (CHOP), and spliced X-box binding protein 1 (XBP1s). The main outcome of UPR signaling, particularly in the early phase, is the restoration of ER homeostasis through inhibition of protein synthesis or upregulation of ER chaperone proteins [9,10]. However, prolonged UPR due to continuous stress can lead to the induction of apoptotic cell death [11,12]. Thus, the UPR is a cellular mechanism that controls cell fate in response to stress.

ER stress and the UPR can also be activated in skeletal muscles that are exposed to metabolic stress, as occurs in diabetic patients [13], or by the consumption of a high-fat diet [14,15]. The high concentration of free fatty acids and especially of saturated fatty acids (SFAs) in plasma under these conditions is one of the main triggers for UPR in skeletal muscle [16–18]. The UPR is closely associated with SFA-induced inflammation, insulin resistance, and apoptosis in skeletal muscle [18–20], indicating there is crosstalk between the UPR and signaling pathways that regulate metabolism [21,22]. The AMP-activated protein kinase (AMPK) pathway is conserved across eukaryotes and integrates signals from multiple sources to control cellular energy balance [23]. Alterations to AMPK also contribute

to the metabolic adaptations and progress of insulin resistance in muscles exposed to SFAs [24]. Given their critical influence on muscle health and metabolism, elucidating the interplay and synergisms (or antagomisms) between AMPK and UPR is prerequisite for the development of novel therapeutics or strategies to ameliorate muscle metabolic disorders. Although there is increasing evidence for interactions between AMPK signaling and the UPR [25–32], the mechanistic basis for crosstalk between these two pathways has yet to be elucidated in different models of ER stress.

Therefore, in the present study we investigated whether there is crosstalk between AMPK signaling and the UPR following induction by palmitate in skeletal muscle cells, as well as the possible underlying mechanism. We found that AMPK was activated in myotubes in response to palmitate treatment. Moreover, we showed that AMPK signaling was associated with early activation of the UPR via a positive feedback mechanism. Additionally, pharmacologic activation of AMPK led to the induction of UPR. These findings provide novel insights into the interactions between metabolic signals and homeostatic mechanisms in skeletal muscle cells that may be perturbed in metabolic disorders.

2. Materials and Methods

2.1 Cell Culture

C2C12 myoblast cells (cat. no. 1101MOUPUMC000099) were purchased from National Infrastructure of Cell Line Resource (NICR) (Beijing, China). This cell line has been authenticated by NICR with flow cytometry. Venor®Gem OneStep Kit (Minerva Biolabs®, Berlin, Germany; cat. no.11-8025) was used to confirm that there is no mycoplasma contamination in C2C12 cells.

Mouse C2C12 myoblast cells were cultured in growth medium containing 89% high-glucose Dulbecco's modified Eagle medium (DMEM) (Gibco, Grand Island, NY, USA), 10% fetal bovine serum (FBS) (Sigma-Aldrich, St. Louis, MO, USA) and 1% Penicillin/Streptomycin at 37 °C in a 5% CO_2 atmosphere. After reaching 80%–90% confluence, the cells were then differentiated into myotubes by replacing the growth medium with differentiation medium (97% high-glucose DMEM, 2% horse serum, 1% Penicillin/Streptomycin) for 4 days.

2.2 Experimental Treatments

Palmitate (Sigma-Aldrich; cat. no. P0500) was dissolved in ethanol and diluted to 500 µmol/L in DMEM containing 2% AlbumiNZ bovine serum albumin (MP Biomedicals, Solon, OH, USA; cat. no. 199896), 2% FBS (Atlanta Biologicals, Flowery Branch, GA, USA), 2 mmol/L L-carnitine (Sigma-Aldrich; cat. no. C0283), and 1% antibiotics [33]. Control C2C12 myotubes were incubated in the same medium except that palmitate was substituted with an equal volume of ethanol. For some treatment conditions, 10 µmol/L compound C (prepared in dimethylsulfoxide [DMSO]; Sigma-Aldrich) was coincubated with palmitate for 12 h. DMSO was also used as a vehicle control for the treatments. To inhibit ER stress, C2C12 myotubes were pretreated for 1 h with 1 mM tauroursodeoxycholic acid (TUDCA) (Millipore, Billerica, MA, USA; cat. no. 580549) before the addition of palmitate for another 12 h. To activate AMPK signaling, the AMPK agonists 5-amino-1-β-D-ribofuranosylimidazole-4-carboxamide (AICAR) (Sigma-Aldrich; cat. no. A9978) or ex229 (Selleckchem; cat. no. S8654) were added to the myotubes at the concentrations shown in the figure legends for different times.

2.3 RNA Interference

Adenoviral constructs containing short hairpin RNA (shRNA) against AMPKα1 (PRKAA1, NM_001013367) or scrambled shRNA (negative control) were constructed by Genechem (Shanghai, China). C2C12 myotubes were transfected with the adenoviral constructs (multiplicity of infection of 100) for 12 h, and then treated with palmitate or left untreated as described above.

2.4 RNA Extraction and Real Time-PCR (RT-PCR)

Total RNA was extracted from C2C12 myotubes using TRIzol reagent (Invitrogen, Carlsbad, CA, USA; cat. no. 15596-026) and then 500 ng of total RNA was reverse transcribed into cDNA using the PrimeScript RT reagent kit (Takara Bio, Otsu, Japan; cat. no. RR037A) according to manufacturer's instructions. RT-PCR was performed using a StepOnePlus RT-PCR system (Invitrogen) with fast SYBR Green Master Mix (Applied Biosystems, Foster City, CA, USA; cat. no. 4385612). Each RT-PCR mixture contained 21 µL sterile water, 25 µL SYBR Green, 2 µL cDNA (500 ng/µL), and 1 µL each of forward and primers (10 pmol/µL). The reaction was performed by an initial denaturation step at 95 °C for 10 min, followed by 40 cycles of denaturation at 95 °C for 10 s, annealing at the melting temperature of the specific primer set for 10 s, elongation at 72 °C for 15 s, and concluded with a melting curve step. Target gene expression levels were normalized to those of the 18S rRNA gene. The sequences of the primers used are listed in **Supplementary Table 1**.

2.5 Immunoblotting

C2C12 myotubes were lysed in RIPA buffer containing 20 mM Tris·HCl (pH 7.4), 150 mM NaCl, 2.5 mM EDTA, 1% Triton X-100, 10% glycerol, 0.1% Sodium dodecyl sulfate (SDS), 1% deoxycholate and 1% protease inhibitor cocktail (Roche, Basel, Switzerland; cat. no. 04693132001). The supernatant was collected by centrifugation at 12,000 ×g for 10 min at 4 °C, and the protein concentration was determined using Bradford protein assay reagents (Bio-Rad, Hercules, CA, USA; cat. no.500-0203). Equal amounts of extracted proteins (30 µg per sample) were denatured in SDS loading buffer and separated

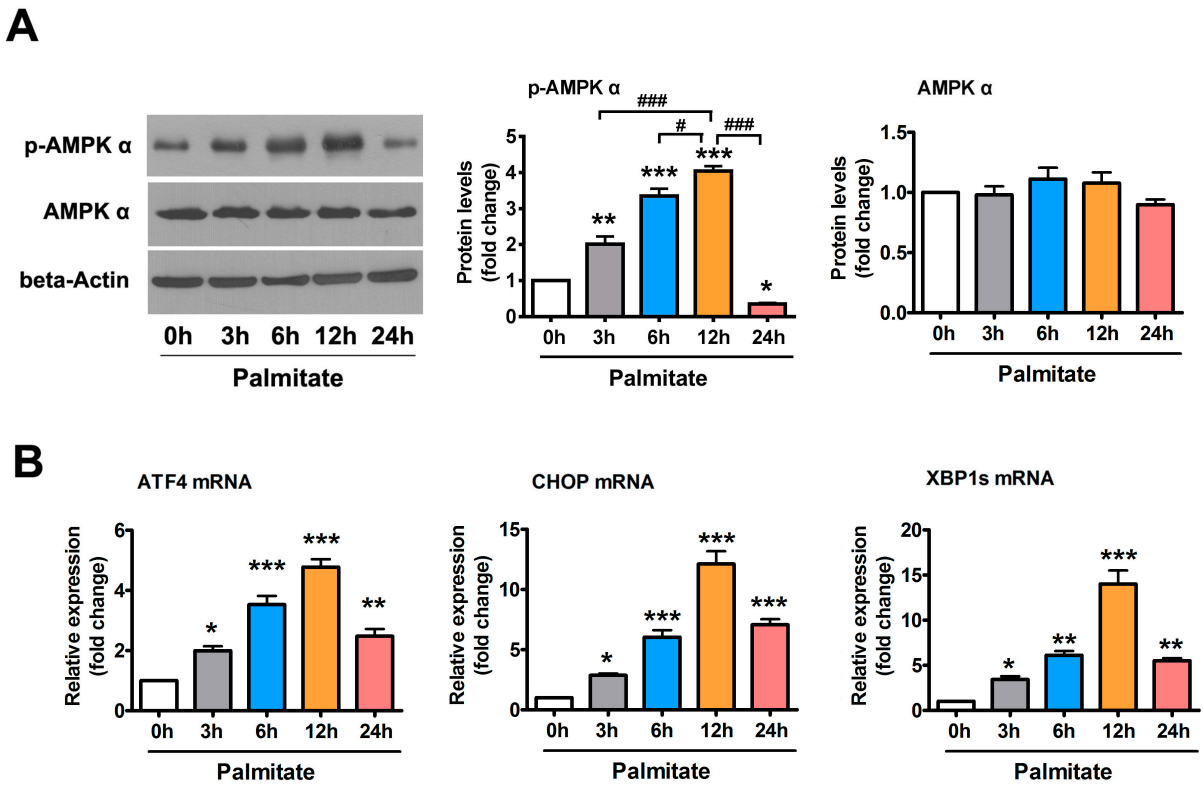

Fig. 1. AMPK signaling is activated within 12 h of palmitate treatment. (A) C2C12 myotubes were incubated with 0.5 mM palmitate for 0, 3, 6, 12, and 24 h. The proteins levels of AMPKα and p-AMPKα were evaluated by Western blot analysis (n = 4). (B) RT-PCR analysis of the mRNA levels for *ATF4*, *CHOP*, and *XBP1*s in C2C12 myotubes treated as described in panel A (n = 4). Data are shown as the mean $\pm$ SD. *$p < 0.05$, **$p < 0.01$, ***$p < 0.001$ vs the control (0 h) group; #$p < 0.05$, ###$p < 0.001$ vs as indicated groups (one-way analysis of variance).

on SDS-polyacrylamide gels. The proteins were then transferred to a nitrocellulose membrane, which was blocked for 2 h in 5% non-fat milk or bovine serum albumin diluted in TBST. The membrane was then incubated overnight at 4 °C with primary antibodies against CHOP (cat. no. 5554), ATF4 (cat. no. 11815), AMPKα (cat. no. 2532), and p-AMPKα (cat. no. 2531) (all from Cell Signaling Technology, Danvers, MA, USA), and β-actin (Santa Cruz Biotechnology, Santa Cruz, CA, USA; cat. no. sc130656). The next day, the membrane was washed 3 times with TBST and incubated for 2 h at room temperature with secondary antibodies in 5% nonfat milk, followed by incubation with enhanced chemiluminescence reagent (Thermo Fisher Scientific; cat. no. 34580) in a dark room. Protein bands were quantified using Image-Pro Plus v6.0 software (Media Cybernetics, Rockville, MD, USA) and the densitometry of the protein signal was normalized to that of β-actin.

2.6 Statistical Analysis

Data are presented as mean $\pm$ SD. One-way or two-way analysis of variance followed by the Tukey's post hoc test was used to compare the means of multiple groups using Prism version 7.0 software (GraphPad, La Jolla, CA, USA). $p \leq 0.05$ was considered statistically significant.

3. Results

3.1 AMPK Signaling is Activated in the Early Stages of the UPR in Myotubes

We investigated the AMPK phosphorylation status and the expression of UPR markers in C2C12 myotubes treated with palmitate (a major component of dietary saturated fats) for different times. While the total AMPKα levels remained constant over time, AMPKα phosphorylation increased after 3 h of palmitate treatment and reached a peak after 12 h. The expression of AMPK phosphorylation after 12 h of palmitate treatment showed a significant difference compared to any other groups. However, after 24 h the p-AMPKα level was lower than in the control group (Fig. 1A). The gene expression level of UPR markers such as *CHOP*, *ATF4*, and *XBP1s* was also upregulated after 3 h of palmitate treatment and peaked at 12 h (Fig. 1B). These results indicate that activation of AMPK signaling induced by palmitate in myotubes is closely associated with the early activation of UPR.

3.2 AMPK Signaling is Involved in Palmitate-Induced UPR in Myotubes

To further investigate the interaction between the AMPK pathway and UPR, C2C12 myotubes were treated

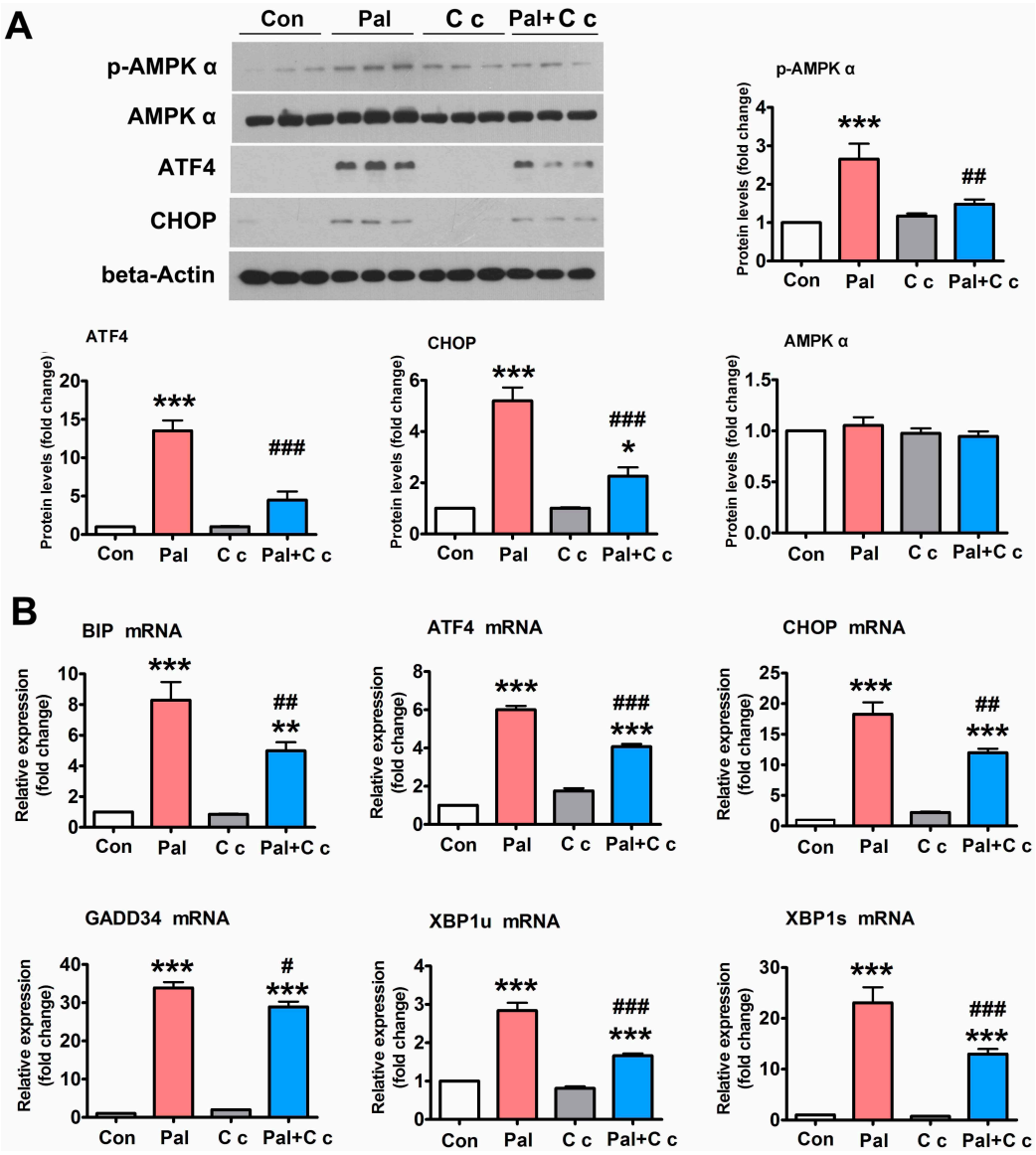

Fig. 2. AMPK inhibition with compound C attenuates palmitate-induced UPR in C2C12 myotubes. (A) Western blot analysis of AMPKα, p-AMPKα, CHOP, and ATF4 proteins levels in C2C12 myotubes treated with 0.5 mM palmitate in the presence or absence of 10 μM of the AMPK inhibitor compound C (n = 6). (B) *BIP*, *ATF4*, *CHOP*, *GADD34*, *XBP1u*, and *XBP1s* mRNA levels were determined by RT-PCR in C2C12 myotubes treated as described in panel A (n = 6). Data are shown as the mean ± SD. *$p < 0.05$, **$p < 0.01$, ***$p < 0.001$ vs control (Con) group; #$p < 0.05$, ##$p < 0.01$, ###$p < 0.001$ vs palmitate (Pal) group (two-way analysis of variance).

with palmitate for 12 h with or without compound C, a widely used specific inhibitor of AMPK. As expected, palmitate caused activation of AMPK, as well as increased expression of the ATF4 and CHOP proteins (Fig. 2A). Compound C completely abolished the AMPK activation induced by palmitate (Fig. 2A) and reduced the palmitate-induced upregulation of ATF4 and CHOP protein levels (Fig. 2A). In agreement with the above findings, palmitate induced the upregulation of gene expression for multiple components of UPR, including *ATF4*, *CHOP*, *GADD34*, chaperone *BIP*, *XBP1u* and *XBP1s* (Fig. 2B). This upregulation was also attenuated by treatment with compound C (Fig. 2B).

To more specifically inhibit the AMPK signaling pathway, C2C12 myotubes were infected with adenovirus that expressed AMPKα shRNA. This confirmed the reduction of both total and phosphorylated AMPKα levels in C2C12 myotubes with or without palmitate treatment (Fig. 3). Moreover, the palmitate-induced upregulation of ATF4 and CHOP was also significantly blocked by knocking down AMPKα (Fig. 3). These data demonstrate that AMPK signaling contributes to early activation of the UPR induced by palmitate.

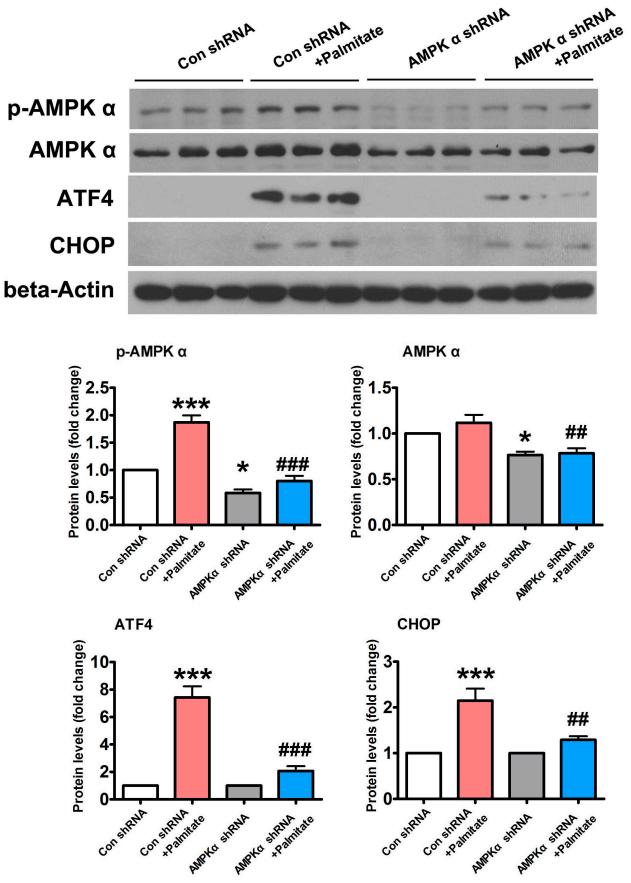

Fig. 3. AMPKα knockdown attenuates palmitate-induced UPR in C2C12 myotubes. C2C12 cells were infected either with control shRNA or AMPKα shRNA for 12 h and then treated with or without 0.5 mM palmitate for a further 12 h. Total protein was then extracted and the protein levels for AMPKα, p-AMPKα, CHOP and ATF4 were evaluated by Western blot analysis (n = 6). All data are shown as the mean $\pm$ SD. *$p < 0.05$, ***$p <$ 0.001 vs Con shRNA group; ##$p < 0.01$, ###$p < 0.001$ vs Con shRNA+Palmitate group (two-way analysis of variance).

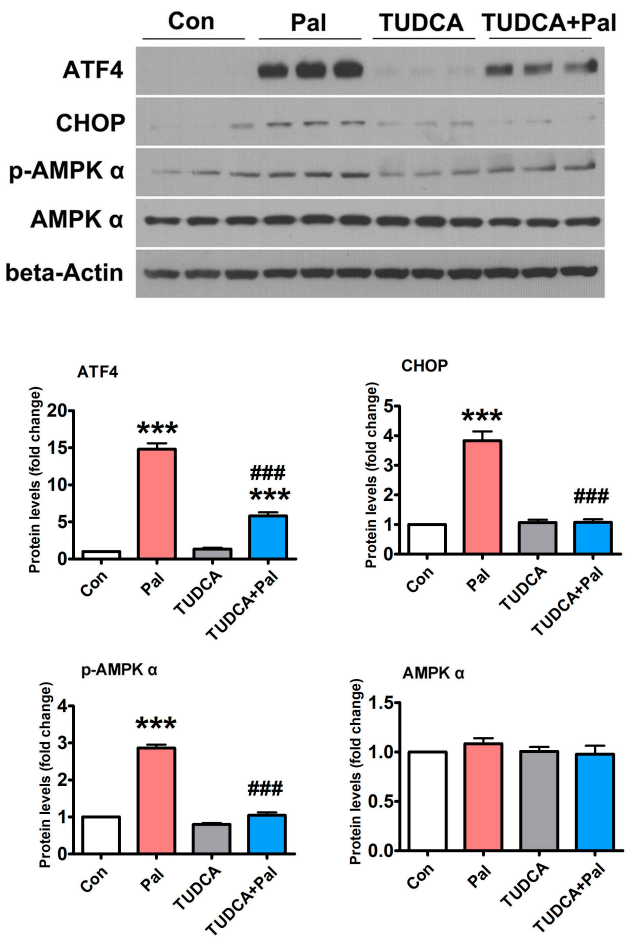

Fig. 4. TUDCA attenuates palmitate-induced AMPK activation in C2C12 myotubes. C2C12 myotubes were pretreated for 1 h with 1 mM TUDCA or left untreated before the addition of palmitate for another 12 h. Protein levels for AMPKα, p-AMPKα, ATF4, and CHOP were evaluated by Western blot analysis (n = 6). Data are shown as the mean $\pm$ SD. ***$p < 0.001$ vs control group; ###$p < 0.001$ vs palmitate group (two-way analysis of variance).

3.3 Inhibition of the UPR with TUDCA Attenuates Palmitate-Induced AMPK Activation

We further investigated whether inhibition of UPR alters AMPK activation in C2C12 myotubes. Myotubes were pretreated with the UPR inhibitor TUDCA for 1 h before the addition of palmitate for 12 h. TUDCA significantly attenuated the palmitate-induced upregulation of ATF4 and CHOP (Fig. 4), thereby demonstrating pharmacologic inhibition of the UPR. Interestingly, TUDCA also abolished palmitate-induced AMPKα phosphorylation (Fig. 4), suggesting a positive feedback loop between the UPR and AMPK pathway in the early stage of palmitate treatment in muscle cells.

3.4 Pharmacologic Activation of AMPK Signaling Induces UPR

Given the finding that AMPK activation contributes to palmitate-induced UPR, we speculated that pharmacologic activation of AMPK would be sufficient to induce the UPR in C2C12 myotubes. To test this hypothesis, C2C12 myotubes were treated with the AMPK agonist AICAR at concentrations ranging from 0.125–2 mM for 12 h to activate AMPK signaling. AMPK phosphorylation increased with increasing AICAR concentration, and was highest at 1 mM AICAR (Fig. 5A). Moreover, ATF4 and CHOP protein levels were upregulated by AICAR in a dose-dependent manner at concentrations <1 mM (Fig. 5A). A higher concentration of AICAR (2 mM) failed to induce AMPK activation and ATF4 and CHOP expression to a greater extent than 1 mM AICAR (Fig. 5A). AICAR was also found to induce gene expression of UPR markers such as *BIP*,

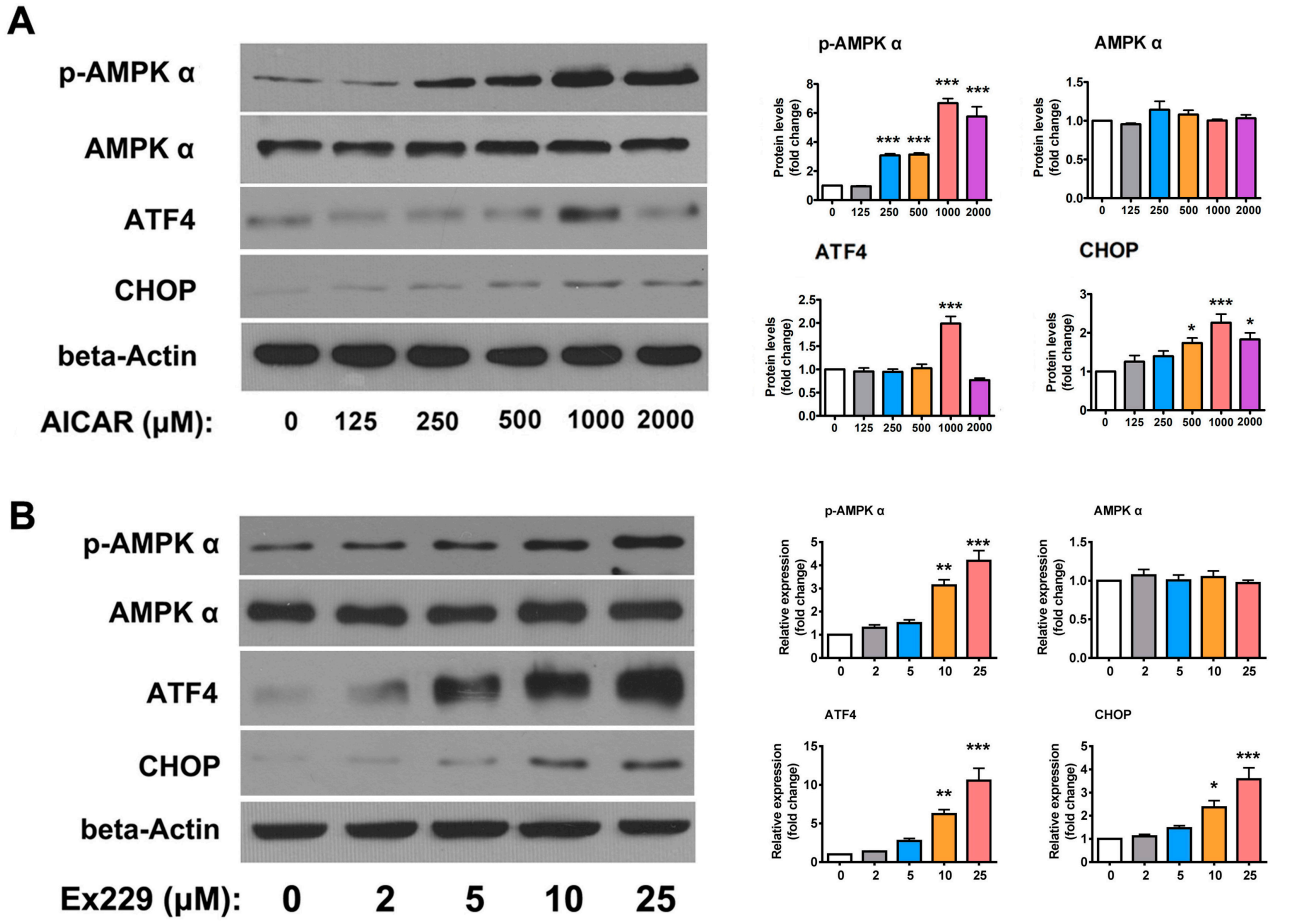

Fig. 5. Pharmacologic activation of AMPK induces UPR. (A) C2C12 myotubes were treated with different concentrations of AICAR (125–2000 μM) for 12 h. The proteins levels for AMPKα, p-AMPKα, ATF4 and CHOP were then determined by Western blot analysis (n = 3). (B) C2C12 myotubes were treated with different concentrations of ex229 (2–25 μM) for 12 h. The proteins levels for AMPKα, p-AMPKα, ATF4 and CHOP were then determined by Western blot analysis (n = 3). Data are shown as the mean ± SD. *$p < 0.05$, **$p < 0.01$, ***$p < 0.001$ vs control (0 μM) group (one-way analysis of variance).

ATF4, and *GADD34* in a dose- and time-dependent manner (**Supplementary Figs. 1,2**). Ex229 is another allosteric activator of the AMPK pathway that is more potent than AICAR [34]. Indeed, ex229 treatment was observed to activate AMPKα phosphorylation at much lower concentrations than AICAR (Fig. 5B). As expected, the protein expression of ATF4 and CHOP was also upregulated by ex229 in a dose-dependent manner (Fig. 5B). Taken together, these results indicate that pharmacologic activation of AMPK is sufficient to induce the UPR in C2C12 myotubes.

4. Discussion

The results of this study provide novel evidence of the interaction between the AMPK pathway and UPR in muscle cells exposed to palmitate, a major component of dietary saturated fats [35]. Specifically, we first observed the unexpected activation of AMPK signaling within 12 h of palmitate treatment, which was accompanied by acute induction of the UPR. In support of these findings, a previous report showed that peroxisome proliferator-activated receptor gamma coactivator (PGC)-1α, one of the main downstream target genes of the AMPK pathway, was transiently upregulated after 4 and 8 h of palmitate treatment [36]. However, another study found that the AMPK pathway was inhibited in cells treated with palmitate for 16 h [18]. We speculate this discrepancy may be due to differences in the duration of treatment, especially since the changes induced by palmitate *in vitro* are stronger and occur more rapidly than those observed during clinical obesity or after induction by a high-fat diet. Indeed, we also found that p-AMPKα was downregulated in cells exposed to palmitate for 24 h.

The association between the UPR and AMPK has been investigated previously [27,37–40]. Several studies on palmitate-induced ER stress have demonstrated an inhibitory effect of AMPK signaling on the UPR in different tissues and cells [27,37,40]. For example, pharmacologic activation of AMPK with AICAR was shown to suppress palmitate-induced ER stress in rat vascular endothelial cells [29]. In C2C12 myotubes, both GW501516

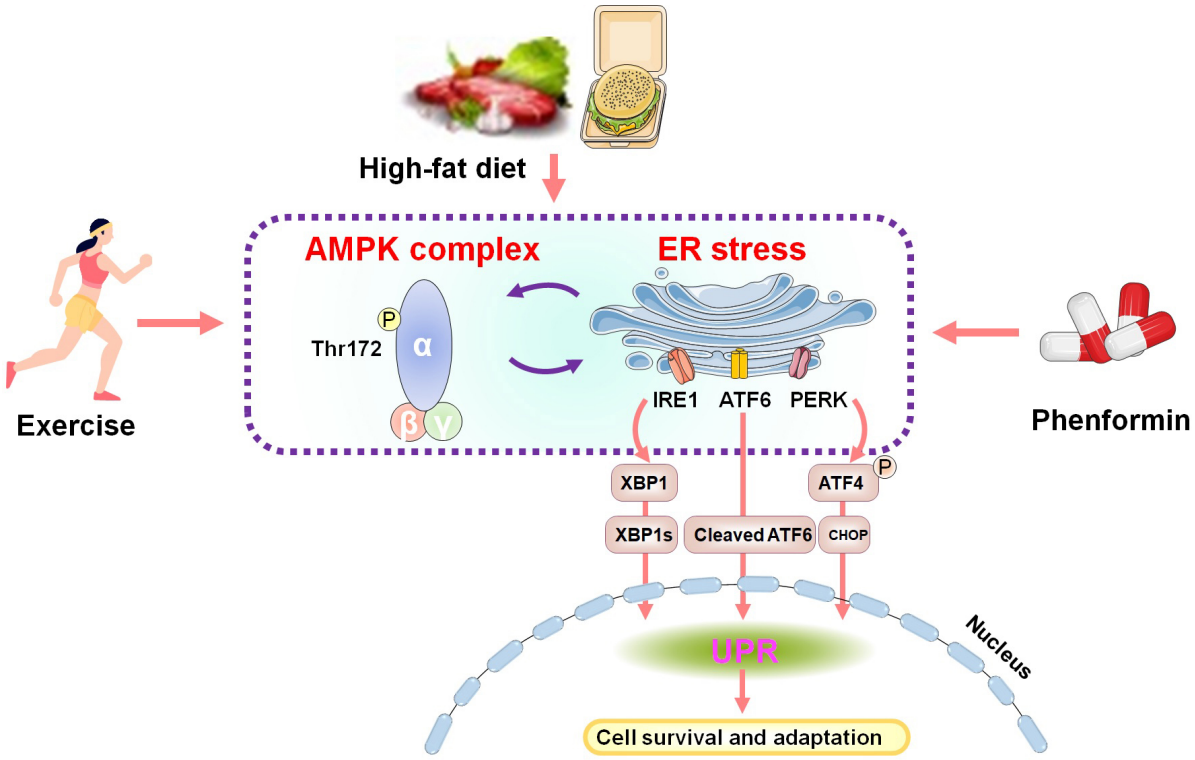

Fig. 6. Bidirectional crosstalk between AMPK signaling and unfolded protein response (UPR) in muscle cells exposed to saturated fatty acids (SFAs). During the early stages after palmitate treatment of muscle cells, AMPK signaling and UPR are activated and crosstalk through a positive feedback mechanism, thereby facilitating restoration of ER homeostasis. Physiological (e.g., exercise) or pharmacological (e.g., phenformin) interventions can accelerate the restoration of ER homeostasis and muscle health by promoting bidirectional crosstalk between AMPK signaling and UPR during the early stages of regular high-fat diet. ER, endoplasmic reticulum.

(a peroxisome proliferator-activated receptor [PPAR]δ receptor agonist) and oleate inhibited palmitate-induced ER stress through an AMPK-dependent mechanism [18,41]. Similarly, 5-lipoxygenase protected C2C12 myotubes from palmitate-induced ER stress via the activation of AMPK [42]. AMPK activation with AICAR (2 mM) effectively reduced palmitate-induced ER stress in muscle cells [18]. However, our results showed that inhibiting the AMPK pathway in myotubes attenuated the UPR induced by palmitate, thus demonstrating a stimulatory effect of the AMPK pathway on palmitate-induced UPR. In agreement with our findings, the antidiabetic drug phenformin was shown to activate ER stress in an AMPK-dependent manner, while AMPK deficiency completely abolished phenformin-induced UPR [43]. Similarly, it was reported that AMPK activation induced mild UPR in C3H10T1/2 mouse mesenchymal stem cells [31]. Moreover, we demonstrated that inhibiting the UPR resulted in mitigation of palmitate-induced AMPK activation, indicating the existence of a positive feedback loop between AMPK and the UPR in the early stages of palmitate treatment in muscle cells. To our knowledge, this is the first report of a positive feedback regulatory mechanism between the AMPK pathway and UPR.

Interestingly, we also found that pharmacologic activation of AMPK with AICAR or ex229 was sufficient to induce upregulation of UPR components in myotubes. In line with this finding, PGC-1α was shown to induce the expression of several UPR-related genes in skeletal muscle [32]. Moreover, ER stress markers (e.g., ATF3 and CHOP) and chaperones (e.g., BIP and GRP94) were significantly unregulated in the gastrocnemius muscle of transgenic mice with muscle-specific overexpression of PGC-1α [32]. PGC-1α overexpression also induced the expression of genes related to protein folding and the UPR in primary myotubes [32]. The increased expression of BIP and GADD34 caused by exercise was abolished in muscle-specific PGC-1α knockout mice, demonstrating that PGC-1α is important for the UPR in skeletal muscle [32]. Given the essential role of PGC-1α as an effector of the AMPK signaling pathway and of its upregulation shortly after palmitate treatment [36], we speculate that PGC-1α is involved in the early activation of palmitate-induced ER stress in skeletal muscle.

5. Conclusions

In summary, we have provided evidence of bidirectional crosstalk between AMPK signaling and early activation of the UPR in muscle cells exposed to SFAs (Fig. 6). We also showed that pharmacologic activation of AMPK was sufficient to induce mild UPR in skeletal muscle cells.

These findings demonstrate an essential role for the AMPK pathway in restoring ER homeostasis via activation of the UPR in response to metabolic stress. Furthermore, they may guide the development of new strategies for the treatment of diseases such as obesity and diabetes through improvements in skeletal muscle metabolism.

Abbreviations

AICAR, 5-amino-1-β-D-ribofuranosylimidazole-4-carboxamide; AMPK, AMP-activated protein kinase; ATF, activating transcription factor; BIP, binding immunoglobulin protein; CHOP, C/EBP homologous protein; DMEM, Dulbecco's modified Eagle medium; DMSO, dimethylsulfoxide; ER, endoplasmic reticulum; ERK, extracellular signal-regulated kinase; FBS, fetal bovine serum; GADD34, DNA damage-inducible protein 34; IRE1, inositol requiring enzyme 1; PERK, PKR-like endoplasmic reticulum kinase; PGC-1α, peroxisome proliferator-activated receptor gamma coactivator-1α; RT, real-time; SFAs, saturated fatty acids; shRNA, short hairpin RNA; TBST, Tris-buffered saline with 0.1% Tween 20; TUDCA, taurourdodeoxycholic acid; UPR, unfolded protein response; XBP1s, X-box binding protein 1 spliced; XBP1u, X-box binding protein 1 unspliced.

Availability of Data and Materials

The datasets used and/or analyzed during the current study are available from the corresponding author on reasonable request.

Author Contributions

PZ and XC designed the research study. JG, LW, WT, ZL, XP, and WL performed the research. PZ, JG, WL, and SL analyzed the data. PZ, JG, LW, and XC wrote the manuscript. All authors contributed to editorial changes in the manuscript. All authors read and approved the final manuscript.

Ethics Approval and Consent to Participate

Not applicable.

Acknowledgment

Not applicable.

Funding

This work was supported by grants from the National Natural Science Foundation of China (81871522, 32171173) and the State Key Laboratory Grant of Space Medicine Fundamentals and Application (SMFA18B01, SMFA20A02).

Conflict of Interest

The authors declare no conflict of interest.

Supplementary Material

Supplementary material associated with this article can be found, in the online version, at https://doi.org/10.31083/j.fbl2808159.

References

[1] Bohnert KR, McMillan JD, Kumar A. Emerging roles of ER stress and unfolded protein response pathways in skeletal muscle health and disease. Journal of Cellular Physiology. 2018; 233: 67–78.

[2] Gallot YS, Bohnert KR. Confounding Roles of ER Stress and the Unfolded Protein Response in Skeletal Muscle Atrophy. International Journal of Molecular Sciences. 2021; 22: 2567.

[3] Maekawa H, Inagi R. Stress Signal Network between Hypoxia and ER Stress in Chronic Kidney Disease. Frontiers in Physiology. 2017; 8: 74.

[4] Qi M, Dang Y, Xu Q, Yu L, Liu C, Yuan Y, *et al*. Microcystin-LR induced developmental toxicity and apoptosis in zebrafish (Danio rerio) larvae by activation of ER stress response. Chemosphere. 2016; 157: 166–173.

[5] Szpigel A, Hainault I, Carlier A, Venteclef N, Batto AF, Hajduch E, *et al*. Lipid environment induces ER stress, TXNIP expression and inflammation in immune cells of individuals with type 2 diabetes. Diabetologia. 2018; 61: 399–412.

[6] Liu CY, Hsu CC, Huang TT, Lee CH, Chen JL, Yang SH, *et al*. ER stress-related ATF6 upregulates CIP2A and contributes to poor prognosis of colon cancer. Molecular Oncology. 2018; 12: 1706–1717.

[7] Ma Y, Brewer JW, Diehl JA, Hendershot LM. Two distinct stress signaling pathways converge upon the CHOP promoter during the mammalian unfolded protein response. Journal of Molecular Biology. 2002; 318: 1351–1365.

[8] Wang P, Li J, Tao J, Sha B. The luminal domain of the ER stress sensor protein PERK binds misfolded proteins and thereby triggers PERK oligomerization. The Journal of Biological Chemistry. 2018; 293: 4110–4121.

[9] Rutkowski DT, Hegde RS. Regulation of basal cellular physiology by the homeostatic unfolded protein response. The Journal of Cell Biology. 2010; 189: 783–794.

[10] Wang BC, Zhang ST, Chen G. Research Progress of the UPR Mechanism and its Effect on Improving Foreign Protein Expression. Protein and Peptide Letters. 2020; 27: 831–840.

[11] Pinkaew D, Chattopadhyay A, King MD, Chunhacha P, Liu Z, Stevenson HL, *et al*. Fortilin binds IRE1α and prevents ER stress from signaling apoptotic cell death. Nature Communications. 2017; 8: 18.

[12] Zhu Y, Xie M, Meng Z, Leung LK, Chan FL, Hu X, *et al*. Knockdown of TM9SF4 boosts ER stress to trigger cell death of chemoresistant breast cancer cells. Oncogene. 2019; 38: 5778–5791.

[13] Liu J, Wu X, Franklin JL, Messina JL, Hill HS, Moellering DR, *et al*. Mammalian Tribbles homolog 3 impairs insulin action in skeletal muscle: role in glucose-induced insulin resistance. American Journal of Physiology. Endocrinology and Metabolism. 2010; 298: E565–E576.

[14] Sun JL, Park J, Lee T, Jeong JH, Jung TW. DEL-1 ameliorates high-fat diet-induced insulin resistance in mouse skeletal muscle through SIRT1/SERCA2-mediated ER stress suppression. Biochemical Pharmacology. 2020; 171: 113730.

[15] Varone E, Pozzer D, Di Modica S, Chernorudskiy A, Nogara L, Baraldo M, *et al*. SELENON (SEPN1) protects skeletal muscle from saturated fatty acid-induced ER stress and insulin resistance. Redox Biology. 2019; 24: 101176.

[16] Ebersbach-Silva P, Poletto AC, David-Silva A, Seraphim PM, Anhê GF, Passarelli M, *et al*. Palmitate-induced Slc2a4/GLUT4 downregulation in L6 muscle cells: evidence of inflammatory and endoplasmic reticulum stress involvement. Lipids in Health and Disease. 2018; 17: 64.

[17] Peng G, Li L, Liu Y, Pu J, Zhang S, Yu J, *et al*. Oleate blocks palmitate-induced abnormal lipid distribution, endoplasmic reticulum expansion and stress, and insulin resistance in skeletal muscle. Endocrinology. 2011; 152: 2206–2218.

[18] Salvadó L, Coll T, Gómez-Foix AM, Salmerón E, Barroso E, Palomer X, *et al*. Oleate prevents saturated-fatty-acid-induced ER stress, inflammation and insulin resistance in skeletal muscle cells through an AMPK-dependent mechanism. Diabetologia. 2013; 56: 1372–1382.

[19] Liong S, Lappas M. Endoplasmic reticulum stress regulates inflammation and insulin resistance in skeletal muscle from pregnant women. Molecular and Cellular Endocrinology. 2016; 425: 11–25.

[20] Reddy SS, Shruthi K, Joy D, Reddy GB. 4-PBA prevents diabetic muscle atrophy in rats by modulating ER stress response and ubiquitin-proteasome system. Chemico-biological Interactions. 2019; 306: 70–77.

[21] Yang B, Qin Q, Xu L, Lv X, Liu Z, Song E, *et al*. Polychlorinated Biphenyl Quinone Promotes Atherosclerosis through Lipid Accumulation and Endoplasmic Reticulum Stress via CD36. Chemical Research in Toxicology. 2020; 33: 1497–1507.

[22] Yao S, Tian H, Miao C, Zhang DW, Zhao L, Li Y, *et al*. D4F alleviates macrophage-derived foam cell apoptosis by inhibiting CD36 expression and ER stress-CHOP pathway. Journal of Lipid Research. 2015; 56: 836–847.

[23] Carling D. AMPK signalling in health and disease. Current Opinion in Cell Biology. 2017; 45: 31–37.

[24] Kjøbsted R, Hingst JR, Fentz J, Foretz M, Sanz MN, Pehmøller C, *et al*. AMPK in skeletal muscle function and metabolism. FASEB Journal. 2018; 32: 1741–1777.

[25] Behera S, Kapadia B, Kain V, Alamuru-Yellapragada NP, Murunikkara V, Kumar ST, *et al*. ERK1/2 activated PHLPP1 induces skeletal muscle ER stress through the inhibition of a novel substrate AMPK. Biochimica et Biophysica Acta. Molecular Basis of Disease. 2018; 1864: 1702–1716.

[26] Hwang HJ, Jung TW, Choi JH, Lee HJ, Chung HS, Seo JA, *et al*. Knockdown of sestrin2 increases pro-inflammatory reactions and ER stress in the endothelium via an AMPK dependent mechanism. Biochimica et Biophysica Acta. Molecular Basis of Disease. 2017; 1863: 1436–1444.

[27] Huang Y, Li Y, Liu Q, Zhang J, Zhang Z, Wu T, *et al*. Telmisartan attenuates obesity-induced insulin resistance via suppression of AMPK mediated ER stress. Biochemical and Biophysical Research Communications. 2020; 523: 787–794.

[28] Jung TW, Kim HC, Abd El-Aty AM, Jeong JH. Maresin 1 attenuates NAFLD by suppression of endoplasmic reticulum stress via AMPK-SERCA2b pathway. The Journal of Biological Chemistry. 2018; 293: 3981–3988.

[29] Li J, Wang Y, Wang Y, Wen X, Ma XN, Chen W, *et al*. Pharmacological activation of AMPK prevents Drp1-mediated mitochondrial fission and alleviates endoplasmic reticulum stress-associated endothelial dysfunction. Journal of Molecular and Cellular Cardiology. 2015; 86: 62–74.

[30] Liu JQ, Zhang L, Yao J, Yao S, Yuan T. AMPK alleviates endoplasmic reticulum stress by inducing the ER-chaperone ORP150 via FOXO1 to protect human bronchial cells from apoptosis. Biochemical and Biophysical Research Communications. 2018; 497: 564–570.

[31] Son HE, Min HY, Kim EJ, Jang WG. Fat Mass and Obesity-Associated (FTO) Stimulates Osteogenic Differentiation of C3H10T1/2 Cells by Inducing Mild Endoplasmic Reticulum Stress via a Positive Feedback Loop with p-AMPK. Molecules and Cells. 2020; 43: 58–65.

[32] Wu J, Ruas JL, Estall JL, Rasbach KA, Choi JH, Ye L, *et al*. The unfolded protein response mediates adaptation to exercise in skeletal muscle through a PGC-1α/ATF6α complex. Cell Metabolism. 2011; 13: 160–169.

[33] Woodworth-Hobbs ME, Hudson MB, Rahnert JA, Zheng B, Franch HA, Price SR. Docosahexaenoic acid prevents palmitate-induced activation of proteolytic systems in C2C12 myotubes. The Journal of Nutritional Biochemistry. 2014; 25: 868–874.

[34] Lai YC, Kviklyte S, Vertommen D, Lantier L, Foretz M, Viollet B, *et al*. A small-molecule benzimidazole derivative that potently activates AMPK to increase glucose transport in skeletal muscle: comparison with effects of contraction and other AMPK activators. The Biochemical Journal. 2014; 460: 363–375.

[35] Cacicedo JM, Benjachareowong S, Chou E, Ruderman NB, Ido Y. Palmitate-induced apoptosis in cultured bovine retinal pericytes: roles of NAD(P)H oxidase, oxidant stress, and ceramide. Diabetes. 2005; 54: 1838–1845.

[36] Coll T, Jové M, Rodríguez-Calvo R, Eyre E, Palomer X, Sánchez RM, *et al*. Palmitate-mediated downregulation of peroxisome proliferator-activated receptor-gamma coactivator 1alpha in skeletal muscle cells involves MEK1/2 and nuclear factor-kappaB activation. Diabetes. 2006; 55: 2779–2787.

[37] Chen C, Kassan A, Castañeda D, Gabani M, Choi SK, Kassan M. Metformin prevents vascular damage in hypertension through the AMPK/ER stress pathway. Hypertension Research. 2019; 42: 960–969.

[38] Varshney R, Varshney R, Mishra R, Gupta S, Sircar D, Roy P. Kaempferol alleviates palmitic acid-induced lipid stores, endoplasmic reticulum stress and pancreatic β-cell dysfunction through AMPK/mTOR-mediated lipophagy. The Journal of Nutritional Biochemistry. 2018; 57: 212–227.

[39] Yang M, Zhang D, Zhao Z, Sit J, Saint-Sume M, Shabandri O, *et al*. Hepatic E4BP4 induction promotes lipid accumulation by suppressing AMPK signaling in response to chemical or diet-induced ER stress. FASEB Journal: Official Publication of the Federation of American Societies for Experimental Biology. 2020; 34: 13533–13547.

[40] Zhang J, Wang Y, Bao C, Liu T, Li S, Huang J, *et al*. Curcumin loaded PEG PDLLA nanoparticles for attenuating palmitate induced oxidative stress and cardiomyocyte apoptosis through AMPK pathway. International Journal of Molecular Medicine. 2019; 44: 672–682.

[41] Salvadó L, Barroso E, Gómez-Foix AM, Palomer X, Michalik L, Wahli W, *et al*. PPARβ/δ prevents endoplasmic reticulum stress-associated inflammation and insulin resistance in skeletal muscle cells through an AMPK-dependent mechanism. Diabetologia. 2014; 57: 2126–2135.

[42] Kwak HJ, Choi HE, Cheon HG. 5-LO inhibition ameliorates palmitic acid-induced ER stress, oxidative stress and insulin resistance via AMPK activation in murine myotubes. Scientific Reports. 2017; 7: 5025.

[43] Yang L, Sha H, Davisson RL, Qi L. Phenformin activates the unfolded protein response in an AMP-activated protein kinase (AMPK)-dependent manner. The Journal of Biological Chemistry. 2013; 288: 13631–13638.